Electronic Supplementary Information

A comprehensive analysis in one run - In-depth conformation studies of protein-polymer chimeras by asymmetrical flow field-flow fractionation

Bibifatima Kaupbayeva,[a,b] Hironobu Murata,[b] Krzysztof Matyjaszewski,[b,c] Alan J. Russell,[a,b,c,d] Susanne Boye,[e]* Albena Lederer[e,f]*

[a]Department of Biological Sciences, Carnegie Mellon University, 4400 Fifth Avenue, Pittsburgh, PA 15213, United States

[b]Center for Polymer-Based Protein Engineering, Carnegie Mellon University, 5000 Forbes Avenue, Pittsburgh, PA 15213, United States

[c]Department of Chemistry, Carnegie Mellon University, 4400 Fifth Avenue, Pittsburgh, PA 15213, United States

[d]Department of Chemical Engineering, Carnegie Mellon University, 5000 Forbes Avenue, Pittsburgh, PA 15213, United States

[e]Center for Macromolecular Structure Analysis, Leibniz-Institut für Polymerforschung Dresden e.V., Hohe Straße 6, Dresden 01069, Germany

[f]Stellenbosch University, Department of Chemistry and Polymer Science, Private Bag X1, Matieland 7602, South Africa

1. Methods

BCA assay. Avidin conjugates (1.0 mg) were dissolved in deionized water and the sample (25 µL) was mixed with bicinchoninic acid (BCA) solution (1.0) and copper (II) sulfate solution (50:1 vol:vol). The solution was incubated at 60°C for 15 min. Absorbance of the sample was recorded at 562 nm using UV-VIS spectrometer. Avidin concentration (wt%) was determined by comparison of the absorbance to a standard curve (native avidin). Estimation of molar mass (MM) of the conjugate. BCA assay gives a concentration and/or wt% of avidin in the conjugate. Expression for molar mass of the conjugate by BCA method was determined as described previously[1]:

(1-X/100)/229.29/(X/100)/64,000 = molar ratio of CBMA units per single conjugate

X is wt% of avidin in the conjugate. Thus, the molar mass of the conjugate = molar ratio of CBMA units × 229.28 g/mol (MM of CBMA) + 64,000 g/mol (MM of avidin).

Asymmetrical flow field-flow fractionation.

AF4-D4 measurements were carried out on an Eclipse DUALTEC system (Wyatt Technology Europe, Germany) with a 10 mM PBS buffer (pH 7.4) as mobile phase and 0.02 % (w/v) NaN_3 to prevent the growth of algae and bacteria. The channel spacer, made of poly(tetrafluoroethylene), was 490 µm in thickness, and the channel dimensions were 26.5 cm in length and 0.6 - 2.1 cm in width. Regenerated cellulose membrane (molecular weight cut-off 10 kDa) was employed as accumulation wall (Superon GmbH, Germany). An Agilent Technologies 1260er series isocratic pump equipped with a vacuum degasser was used to control the flow rates. The detection system consisted of a MALLS detector (DAWN HELEOS II, Wyatt Technology Europe, Germany) operating at a wavelength of 659 nm with online DLS detector (QELS module, Wyatt

Technologies, USA) which is an add-on unit connected to the 99° angle of the MALLS, a variable wavelength detector (Agilent Technologies, UK) set to 280 nm and an absolute refractive index (RI) detector (Optilab T-rEX, Wyatt Technology Europe GmbH, Germany) operating at a wavelength of 658 nm. All injections were performed with an autosampler (1260 series, Agilent Technologies Deutschland GmbH). The sample concentration was about 1 mg mL^{-1} and the inject load was 50 and 200 µL, respectively. The data collection and calculation of molar masses and radii were performed by Astra 7.3.219 software (Wyatt Technologies, USA). Cross flow rate (F_x) profile was optimized to achieve optimal separation. The channel flow rate (F_c) was set to 0.8 mL min-1 for all AF4 operations. Samples were injected during the focusing/relaxation step within 5 min. The focus flow (F_f) was set at 3 ml min-1. The F_x rate during the elution step was optimized by an exponential gradient of 3 – 0.15 mL min-1 in 30 min. The angular dependencies of scattering intensity were fitted by Debye for initial polymers and Berry plot for conjugates. The refractive index increment dn/dc was determined by manual injection into the RI detector of the samples with varied concentrations. Dn/dc values were determined for all different ligand and conjugate types.

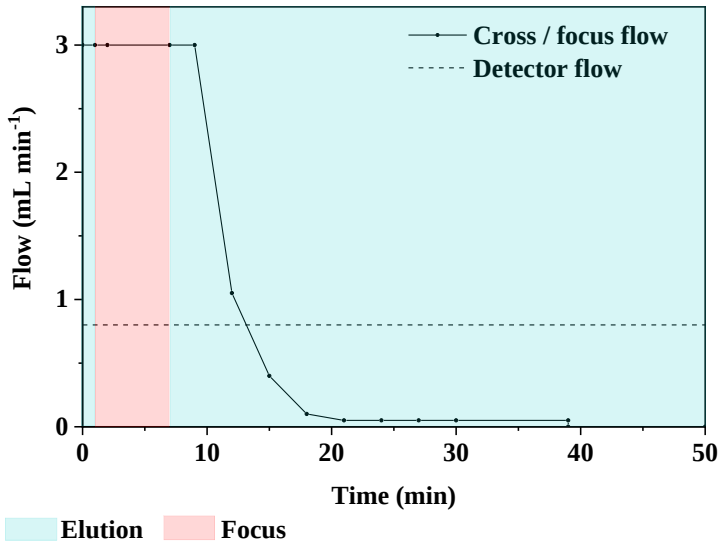

Figure S1. Optimized flow profile for AF4 separation

2. Data and figures

2.1. Initial polymer ligands

Table S1. Comparison of SEC and AF4-D4 results of native avidin, CBMA and OEGMA polymers, single-grafted polymers results were published in Ref.[3] (S-single-headed; D – double-headed)

		AF4-D4							SEC	
	Sample	**dn/dc** (ml g^{-1})	**M_n** (kg mol^{-1})	**M_w** (kg mol^{-1})	**Đ** (M_w/M_n)	**R_g** (nm)	**R_h** (nm)	**Recov-eries** (%)	**$M_{n,SEC}$**[a] (kg mol^{-1})	**Đ**[b] (M_w/M_n)
	Native avidin	0.184	67.2	67.2	1.001	3.7± 0.6	3.5 ± 0.2	83	N.A.	N.A.
F1	**S-pCBMA$_{short}$**	0.154	40.0	49.5	1.24	n.d.	6.8 ± 1.4	81	20.6	1.41
F2	**S-pCBMA$_{long}$**	0.154	107	134	1.25	13.9 ± 1.4	9.4 ± 0.8	90	49.3	1.55
F3	**S-pOEGMA$_{short}$**	0.129	64.6	71.8	1.10	n.d	10.5 ± 3.0	91	24.6	1.26
F4	**S-pOEGMA$_{long}$**	0.129	166	189	1.14	13.1 ± 1.3	10.9 ± 1.0	81	49.5	1.35
F5	**D-pOEGMA$_{short}$**	0.137	99.8	121	1.21	13.9 ± 1.4	10.8 ± 1.4	78	N.A.	N.A.
F6	**D-pOEGMA$_{long}$**	0.137	290	365	1.26	20.0 ± 2.0	14.4 ± 1.1	84	N.A.	N.A.

[a] determined by SEC analysis. [b] Calculated from M_n and M_w of cleaved polymer.

2.2. MALDI-ToF MS of ATRP initiator modified avidin

MALDI-ToF quantification of single-headed ATRP initiator modified avidin

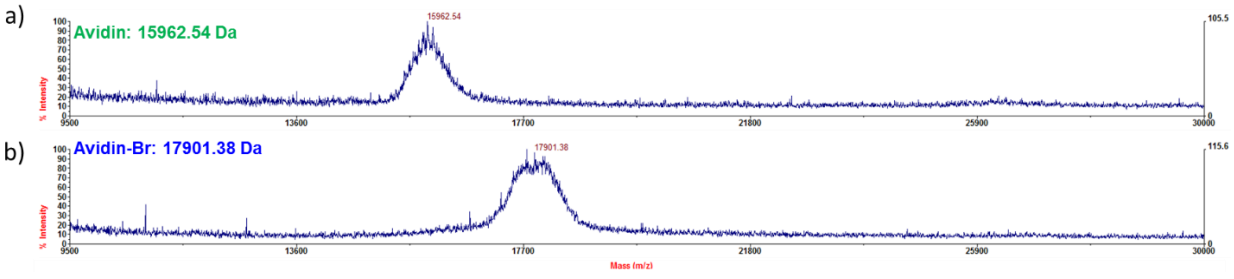

Figure S2. MALDI-ToF mass spectroscopy of native avidin and single-headed initiator modified avidin; a) native avidin; b) avidin-initiator conjugate (8.8 initiators per avidin monomer). Number of modifications was determined by subtracting m/z of native avidin from m/z avidin-single headed initiator conjugates and dividing by the initiator molar mass without the NHS group (220 Da). Total number: **35.2** single-headed initiators per avidin molecule.

MALDI-ToF quantification of double-headed ATRP initiator modified avidin

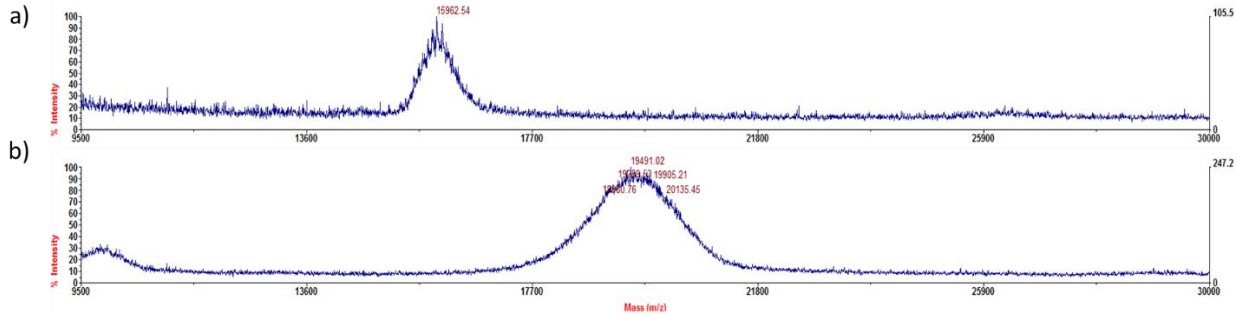

Figure S3. MALDI-ToF mass spectroscopy of native avidin and double-headed initiator modified avidin; a) native avidin; b) avidin-initiator conjugate (7.3 double-headed initiators per avidin monomer). Number of modifications was determined by subtracting m/z of native avidin from m/z avidin-double headed initiator conjugates and dividing by the initiator molar mass without the NHS group (483 Da). Total number: **29.2** double-headed initiators per avidin molecule, in average **58** polymers can be grown from avidin.

2.3. Avidin-polymer conjugates

Table S2. SEC, BCA assay and DLS characterizations of avidin-polymer conjugates, single-grafted conjugates were published in Ref.[3].

		Cleaved polymer M_n[a] (kg mol^{-1})	Cleaved polymer M_w[a] (kg mol^{-1})	Cleaved polymer $Đ$[a]	Cleaved polymer DP[a]	Estimated conjugate molar mass[b] (kg mol^{-1})	Conjugate molar mass[c] (kg mol^{-1})	Polymer DP[c]	R_h[d] (nm)	PDI[d]
					Zwitterionic polymers					
C1	**Single-grafted avi-pCBMA$_{short}$**	9.4	15.3	1.63	41	372	303	32	9.1 ± 1.0	0.48
C2	**Single-grafted avi-pCBMA$_{long}$**	39.4	59.5	1.51	172	1330	525	62	14.9 ± 0.7	0.22
C3	**Double-grafted avi-pCBMA$_{short}$**	4.9	6.1	1.25	21	352	301	17	7.8 ± 0.5	0.47
C4	**Double-grafted avi-pCBMA$_{long}$**	47.2	79.8	1.69	206	2720	406	26	12.7 ± 0.9	0.26
					Neutral polymers					
C5	**Single-grafted avi-pOEGMA$_{short}$**	9.3	14.3	1.54	19	369	291	14	9.9 ± 1.4	0.43
C6	**Single-grafted avi-pOEGMA$_{long}$**	51.8	74.1	1.43	104	1730	485	26	15.5 ± 1.0	0.18
C7	**Double-grafted avi-pOEGMA$_{short}$**	10.5	17.1	1.63	21	666	363	10	10.3 ± 1.0	0.31
C8	**Double-grafted avi-pOEGMA$_{long}$**	98.6	260	2.64	197	5600	622	19	18.2 ± 4.8	0.28

[a] determined by SEC analysis. [b] calculated from M_n of cleaved polymer. [c] estimated by BCA protein assay. [d] determined by batch DLS, number mean average.

2.4. Dynamic light scattering experiments in batch

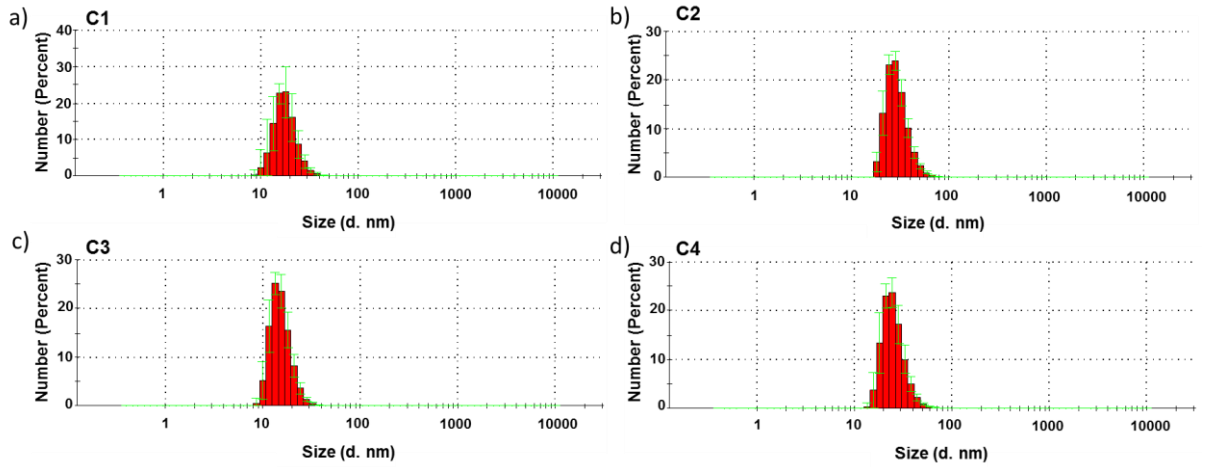

Figure S4. Particle size distribution (number fractions) in batch of zwitterionic avidin-pCBMA conjugates; a) C1; b) C2; c) C3 and d) C4. Conjugates were dissolved at 1 mg mL^{-1} concentration using 0.01 M PBS buffer, pH 7.4. Hydrodynamic diameters were measured three times (5 run each measurement) at room temperature.

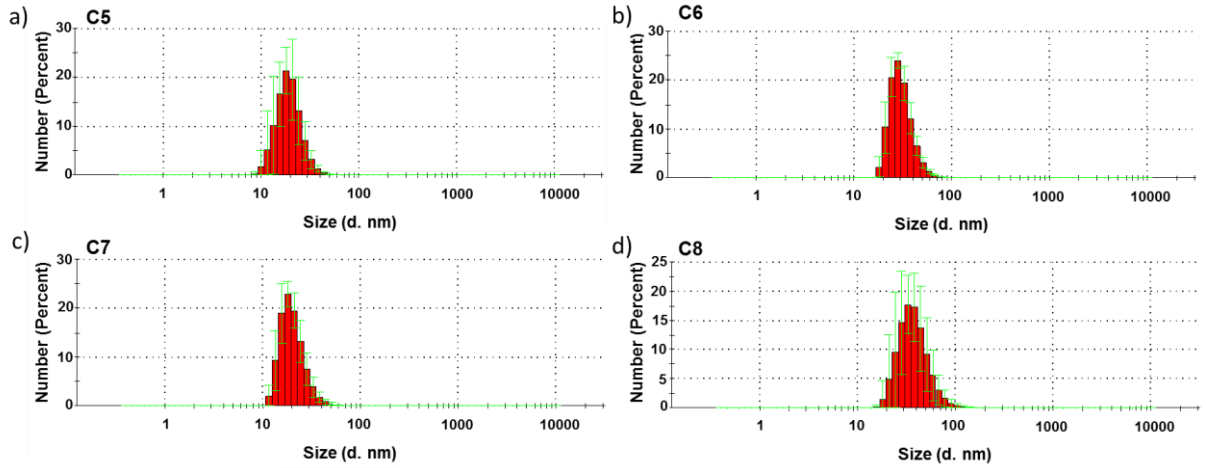

Figure S5. Particle size distribution (number fractions) in batch of neutral avidin-pOEGMA conjugates; a) C5; b) C6; c) C7 and d) C8. Conjugates were dissolved at 1 mg mL^{-1} concentration using 0.01 M PBS buffer, pH 7.4. Hydrodynamic diameters were measured three times (5 run each measurement) at room temperature.

2.5.AF4-LS studies and conformation properties

2.5.1. Short theoretical background for AF4-LS interpretation

Scaling parameter: by plotting R_g vs M, ν can be determined by the slope of the plot, it gives information about the molecular shape in the used solvent

$R_g = K \cdot M^{\nu}$

ν = 0.33 → spheres

ν = 0.5 - 0.6 → random coil macromolecule

ν = 1 → rigid rod

Apparent density: gives information about molecular density, is calculated by R_g and M_w (with V as volume fraction, α as geometrical correction, N_A as Avogadro's number):

$$d_{app,i} = \frac{M_i}{V\,(R_g)_i \cdot N_A} \cdot \alpha \qquad \text{with} \qquad \alpha = \frac{V_{sphere}(R_g)}{V_{sphere}(R)} = \frac{{R_g}^3}{R^3} = \frac{\left(\sqrt{\frac{3}{5}} \cdot R\right)^3}{R^3} = \left(\frac{3}{5}\right)^{\frac{3}{2}}$$

ρ parameter: The ratio between R_g and R_h delivers valuable information about conformation and shape of molecules, some examples[4]:

Homogenous sphere:	0.775
Random coil, linear chain (good solvent):	1.78
Hyperbranched polymer:	1.23
Rod (axial ratio = 2.5):	2.1

2.5.2. AF4 fractograms

Polymers:

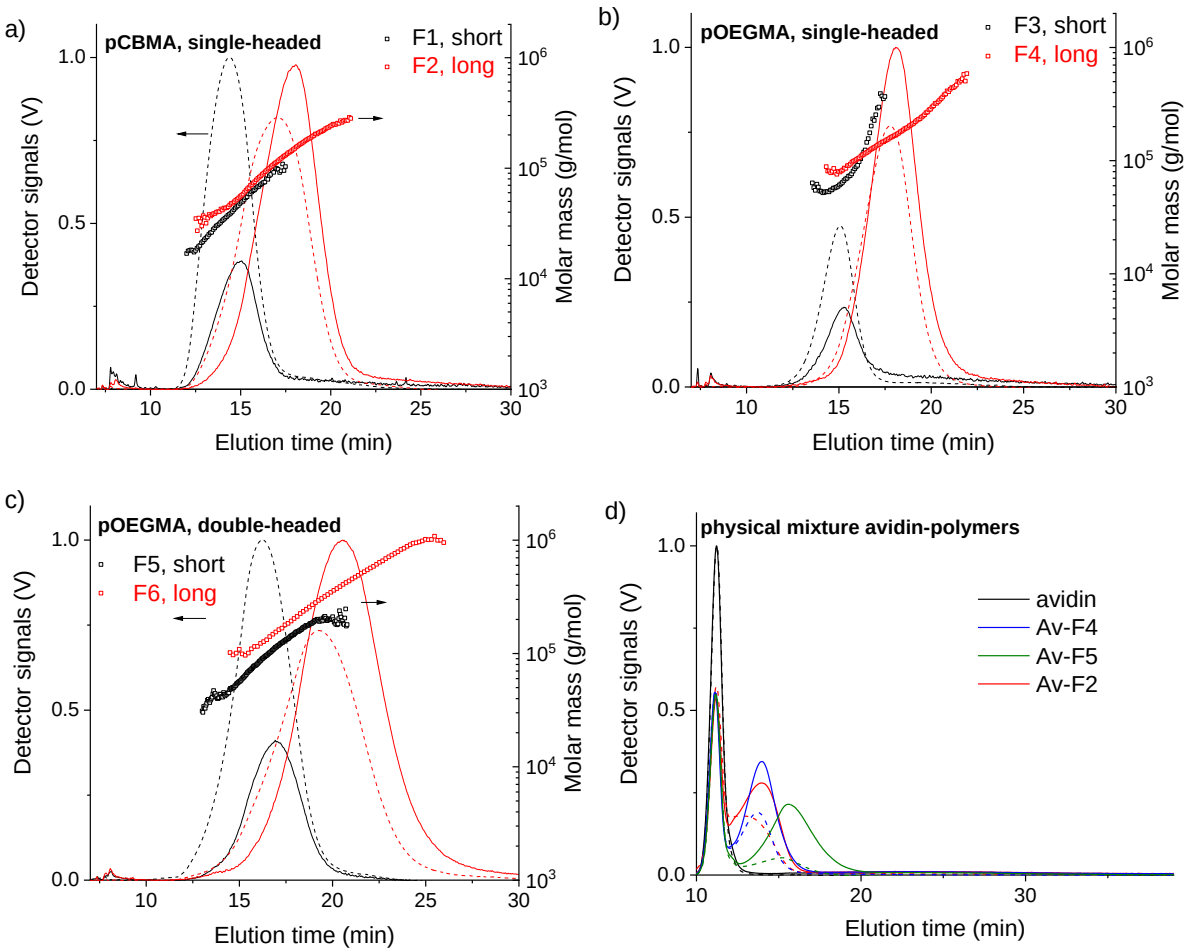

Figure S6. AF4-D4 fractograms of a) short (F1, black) and long (F2, red) single-grafted, zwitterionic pCBMA ligands b) short (F3, black) and long (F4, red) single-grafted, neutral pOEGMA ligands and c) double-grafted, neutral pOEGMA ligands with short (F5, black) and long (F6, red); LS (90°) detector signals (solid line), RI detector signals (dashed line) and molar masses (symbols) vs. elution time and d) fractograms of physical mixtures of native avidin and F2 (red), F4 (blue) and F5 (olive).

Conjugates:

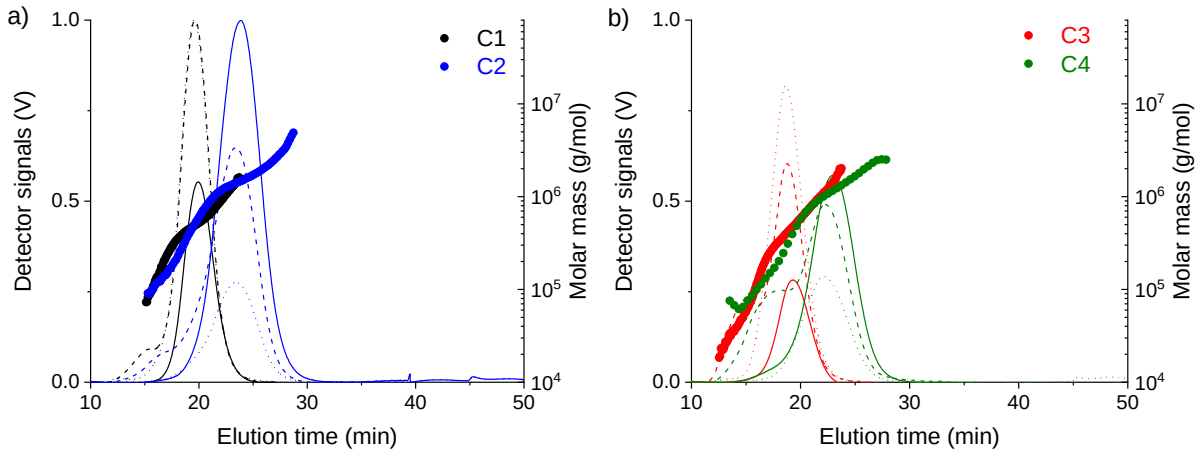

Figure S7. AF4-D4 fractograms of a) single-grafted, zwitterionic avidin-pCBMA conjugates with short (C1, black) and long (C2, blue) polymer ligands b) double-grafted, zwitterionic avidin-pCBMA conjugates with short (C3, red) and long (C4, olive) polymer ligands; molar masses (symbols), LS (90°) detector signals (solid line), RI detector signals (dashed line) and UV (280 nm) detector signals (dotted line) vs. elution time.

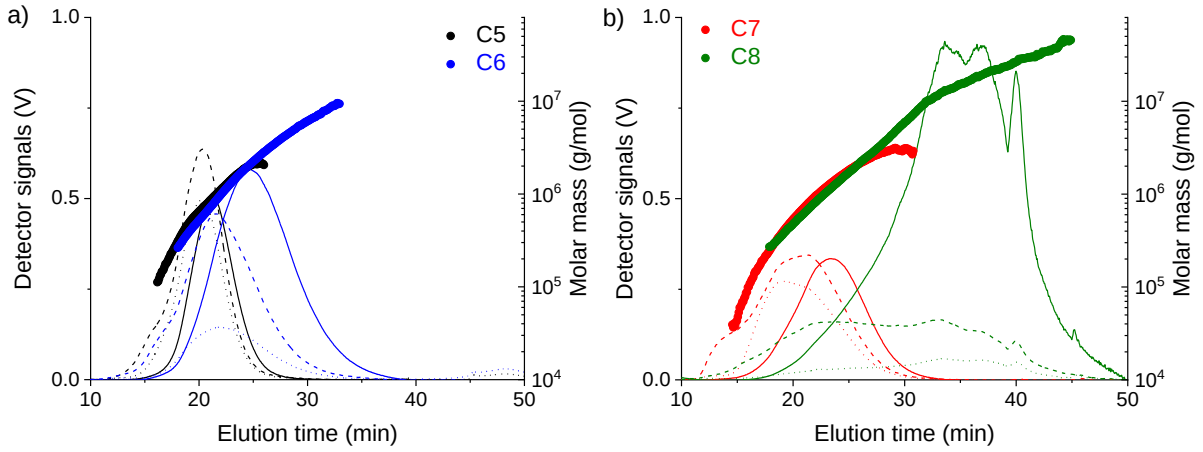

Figure S8. AF4-D4 fractograms of a) single-grafted, neutral avidin-pOEGMA conjugates with short (C5, black) and long (C6, blue) polymer ligands b) double-grafted, neutral avidin-pOEGMA conjugates with short (C7, red) and long (C8, olive) polymer ligands; molar masses (symbols), LS (90°) detector signals (solid line), RI detector signals (dashed line) and UV (280 nm) detector signals (dotted line) vs. elution time.

2.5.3. Conformation studies by AF4-D4

Polymers:

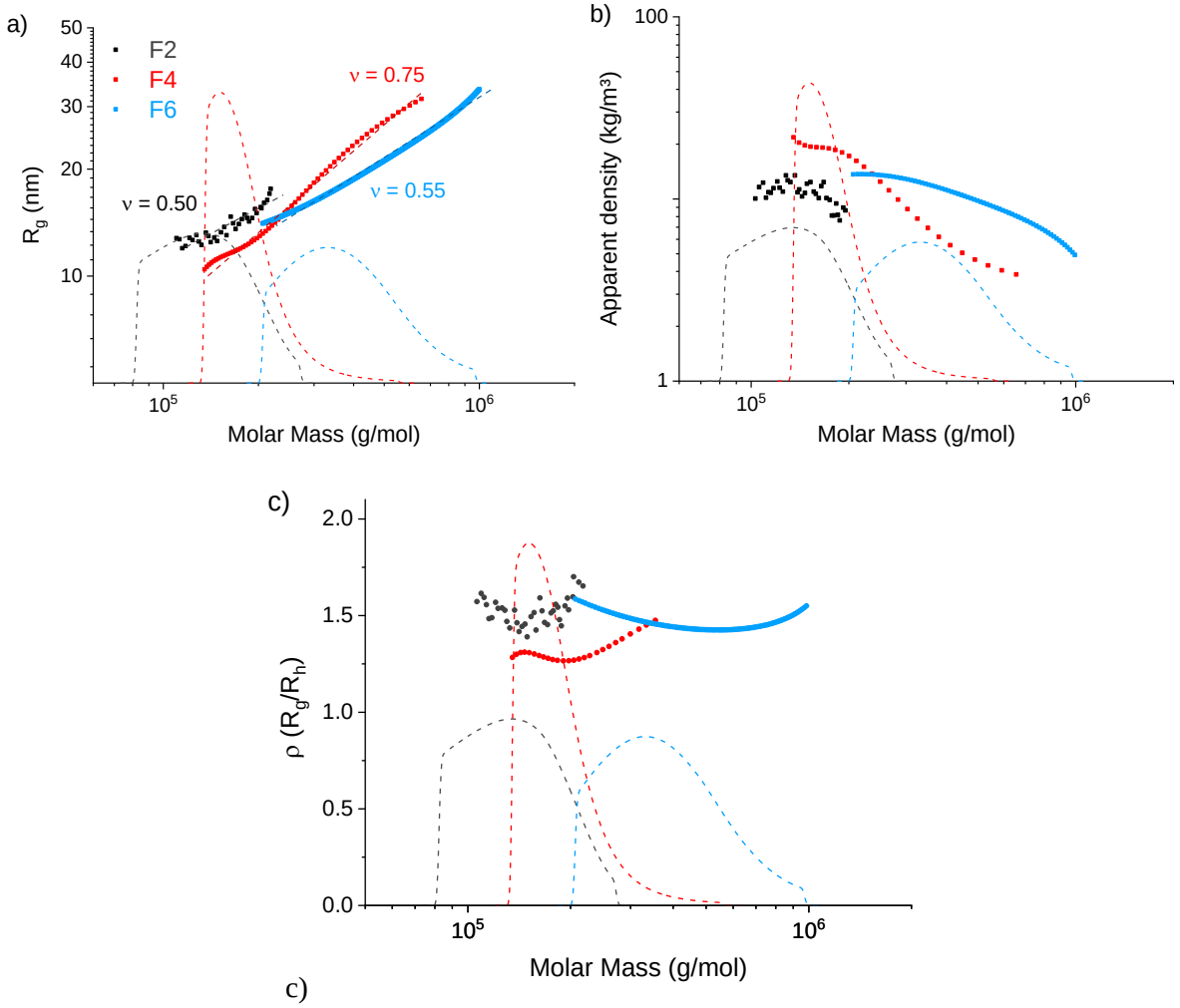

Figure S9. Conformation studies by AF4-D4 of long, zwitterionic pCBMA (F2, dark grey); long, neutral pOEGMA (F4, red) and long, double-headed neutral pOEGMA (F6, blue) ; differential weight fractions (dashed lines) and a) scaling plot R_g and molar mass distributions; b) apparent densities and c) ρ (R_g/R_h) parameter vs. molar masses.

Conjugates of avidin and single-grafted, zwitterionic pCMBA:

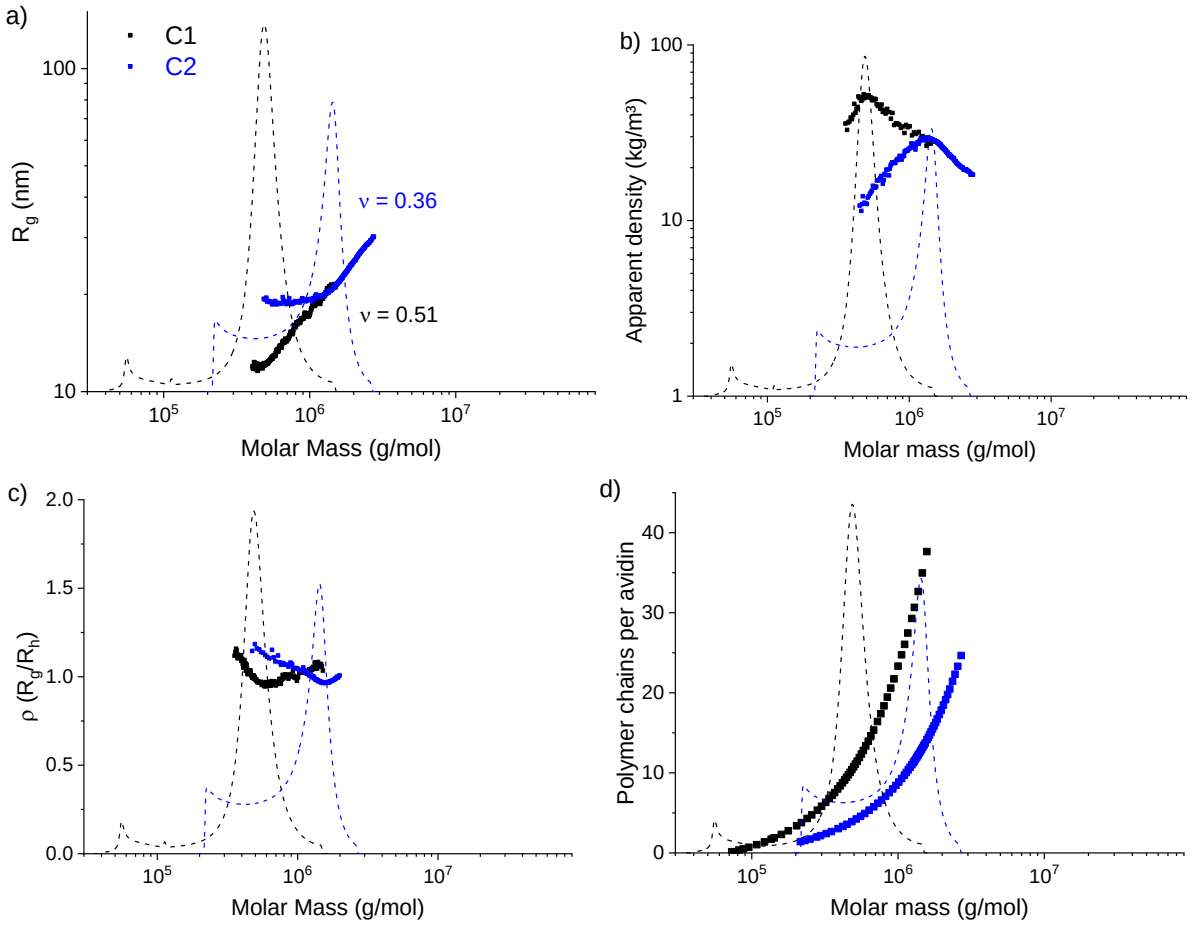

Figure S10. Conformation studies by AF4-D4 of single-grafted, zwitterionic avidin-pCBMA conjugates with short (C1, black) and long (C2, blue) polymer ligands; differential weight fractions (dashed lines) and a) scaling plot R_g and molar mass distributions; b) apparent densities; c) ρ (R_g/R_h) parameter and d) polymer chains per avidin (symbols, calculated by M_n of polymer) vs. molar masses.

Conjugates of avidin and double-grafted, zwitterionic pCMBA:

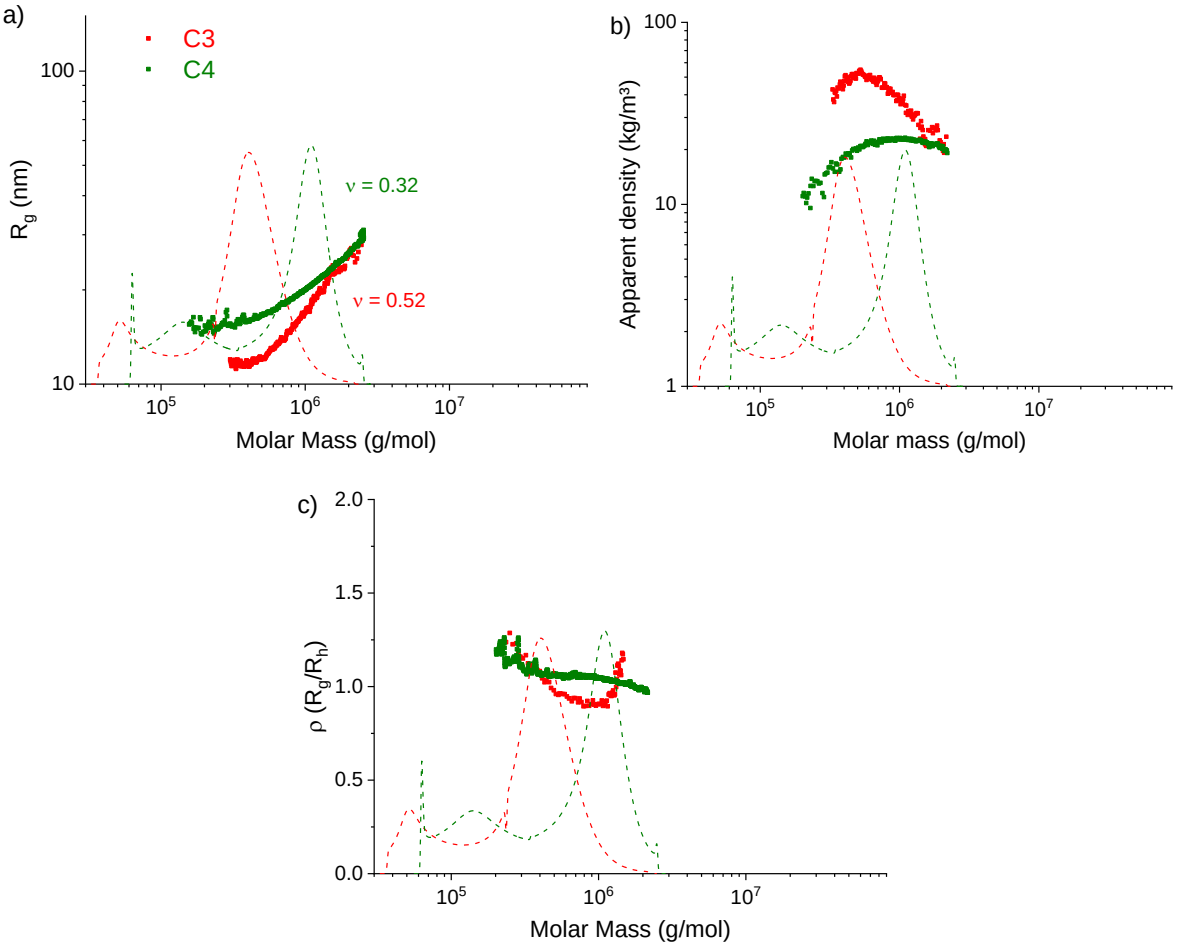

Figure S11. Conformation studies by AF4-D4 of double-grafted, zwitterionic avidin-pCBMA conjugates with short (C3, red) and long (C4, olive) polymer ligands; differential weight fractions (dashed lines) and a) scaling plot R_g and molar mass distributions; b) apparent densities; and c) ρ (R_g/R_h) parameter vs. molar masses.

Conjugates of avidin and single-grafted, neutral pOEGMA:

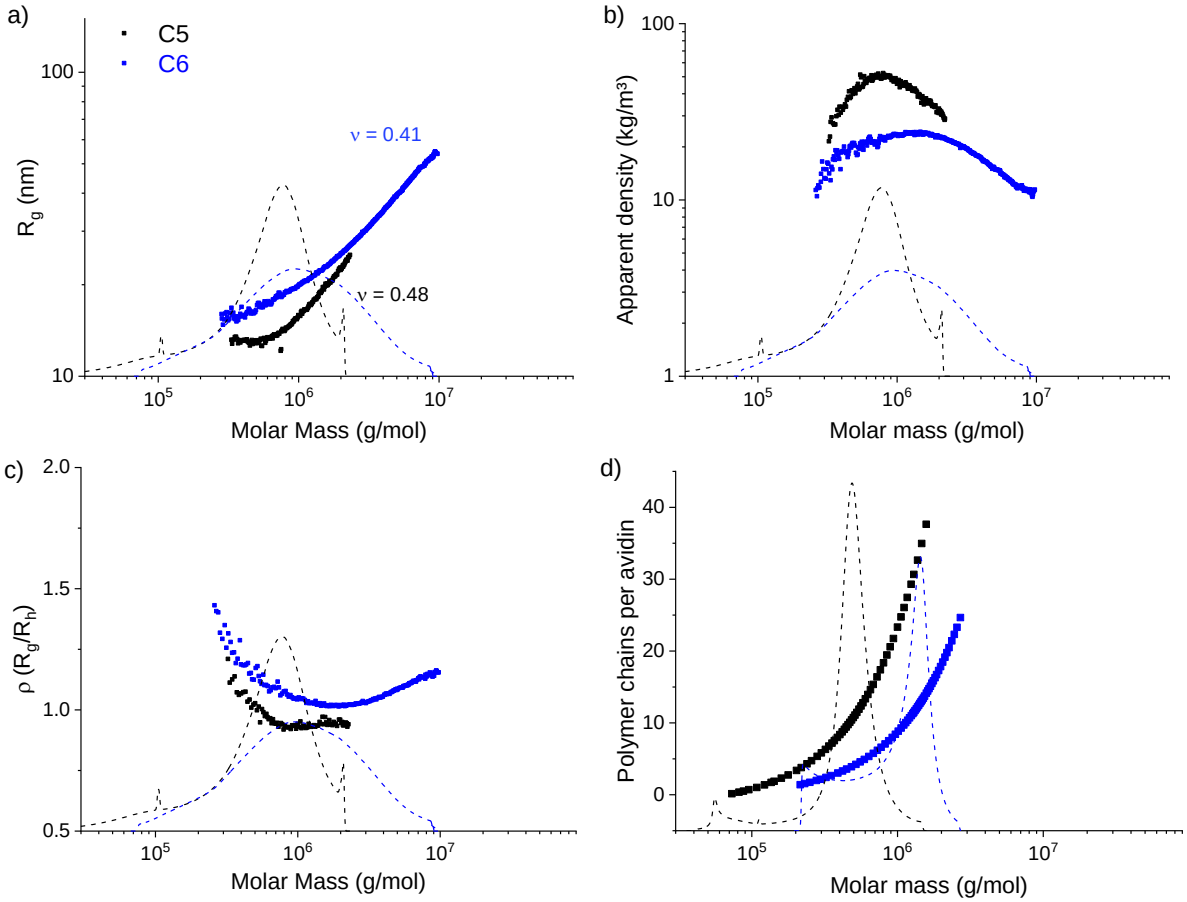

Figure S12. Conformation studies by AF4-D4 of single-grafted, neutral avidin-pOEGMA conjugates with short (C5, black) and long (C6, blue) polymer ligands; differential weight fractions (dashed lines) and a) scaling plot R_g and molar mass distributions; b) apparent densities; c) ρ (R_g/R_h) parameter and d) polymer chains per avidin (symbols, calculated by M_n of polymer) vs. molar masses.

Conjugates of avidin and double-grafted, neutral pOEGMA:

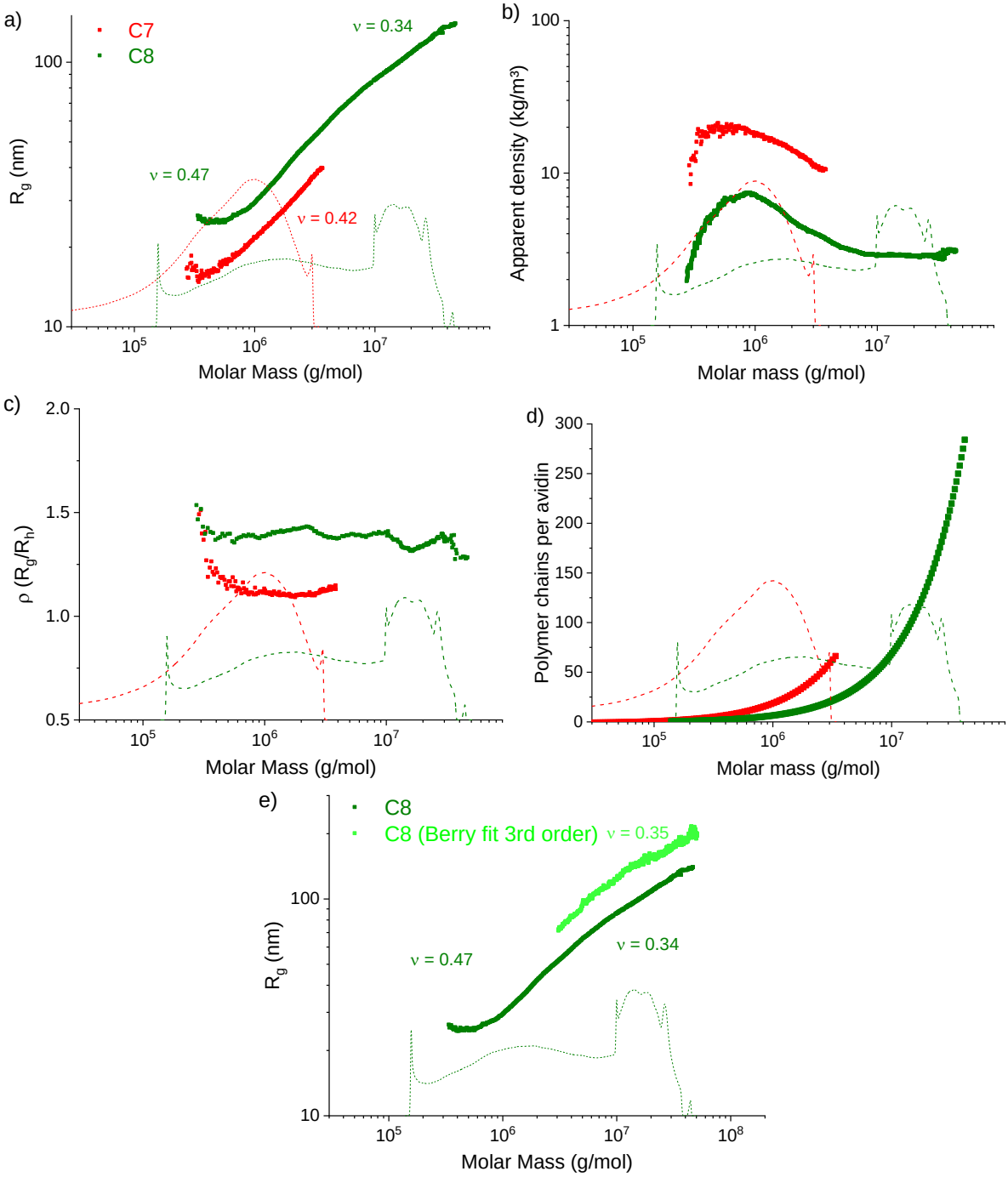

Figure S13. Conformation studies by AF4-D4 of double-grafted, neutral avidin-pOEGMA conjugates with short (C7, red) and long (C8, olive) polymer ligands; differential weight fractions (dashed lines) and a) scaling plot R_g and molar mass distributions; b) apparent densities; c) ρ (R_g/R_h) parameter; d) polymer chains per avidin (symbols, calculated by M_n of polymer) and e) scaling plots R_g and molar mass distribution of C8 with Berry plot first (olive symbols) and third (light green) order fit vs. molar masses.

Comment: Generally, the angular dependencies for molecules with R_g higher than 30 nm can be fitted higher degree. For a better comparability, we decided to perform the Berry fitting for all samples with 1st order degree. Samples C1 to C7 are all below 35 nm and the Fit R² was about 0.998. In case of higher radii of C8 the Fit R² was about 0.996 instead of 0.998 in case of using 3rd fit degree. Especially, in case of broadly distributed conjugate C8, it is challenging

to select limits where to change the fit order because of present shift in radii to higher values visible in Figure S13e without significant change in conformation.

Comparison AF4-MALS and SEC-MALS

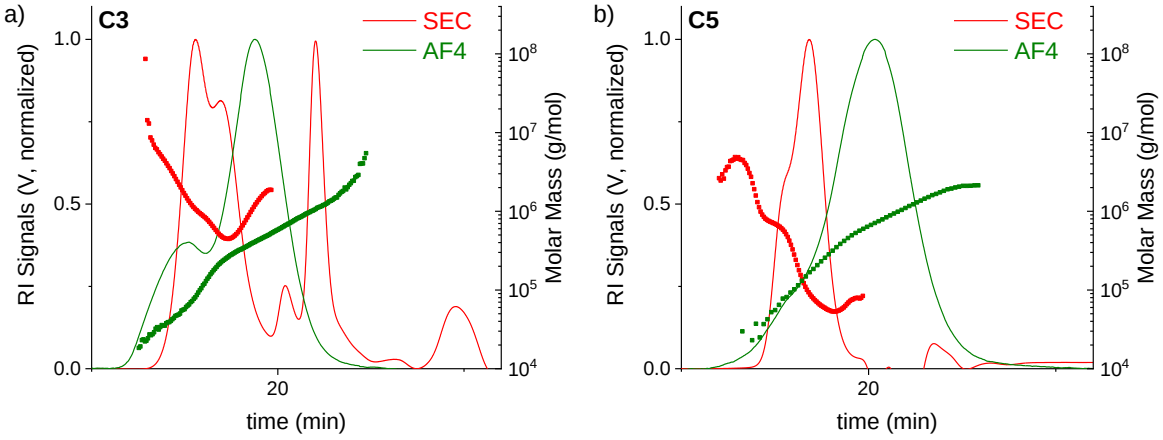

Figure S14. a) RI signals and molar masses vs elution time of C3 (Double-grafted avi-pCBMA$_{short}$) determined by AF4-MALS (green) and SEC-MALS (red). b) RI signals and molar masses vs elution time of C5 (Single-grafted avi-pOEGMAshort) determined by AF4-MALS (green) and SEC-MALS (red).

Comments: The comparative SEC-MALS measurements (Figure S14) were performed using Agilent 1260 Infinity II system (Santa Clara, CA, USA) equipped with Waters Ultrahydrogel Linear column (Milford, MA, USA) and coupled with variable wavelength detector (1260 Infinity II), MALS (DAWN ambient, Wyatt Technology, USA), DLS (Wyatt-QELS, integrated DLS for DAWN), viscometer (Viscostar), and dRI detectors (Optilab). Phosphate-buffer Saline (PBS, pH 7.4) was used as an eluent. The sample concentration was about 2 mg mL^{-1} and the injection load was 100 µL.

Molar masses vs elution volume determined using SEC show clear decomposition of the conjugates to several components and adsorption of the different components to the column material leading to non-enthalpic separation. Such effects can lead to significant misinterpretation of the conjugate structure.

The advantage of AF4-MALLS is that it is a channel-based separation technique and unlike SEC does not have sample-column interactions and has reduced shear forces. The nature of the AF4, with the separation and flow profiles customized for each sample, allows separation and resolution of different conformations without decomposition. Furthermore, the detector signal quality can be improved by varying the sample load. In SEC, "column shedding" can occur if the sample load is too high. Furthermore, co-elution of different conformations with the same molar mass is a common problem that occurs in SEC. However, this phenomenon can be circumvented by varying the flow and separation profile in AF4. This allows for most accurate characterization of the sample's true nature.

References

(1) Murata, H.; Cummings, C. S.; Koepsel, R. R.; Russell, A. J. Polymer-Based Protein Engineering Can Rationally Tune Enzyme Activity, PH-Dependence, and Stability. *Biomacromolecules* **2013**, *14* (6), 1919–1926. https://doi.org/10.1021/bm4002816.

(2) Kaupbayeva, B.; Murata, H.; Lucas, A.; Matyjaszewski, K.; Minden, J. S.; Russell, A. J. Molecular Sieving on the Surface of a Nano-Armored Protein. *Biomacromolecules* **2019**, *20* (3), 1235–1245. https://doi.org/10.1021/acs.biomac.8b01651.

(3) Murata, H.; Baker, S. L.; Kaupbayeva, B.; Lewis, D. J.; Zhang, L.; Boye, S.; Lederer, A.; Russell, A. J. Ligands and Characterization for Effective Bio-Atom-Transfer Radical Polymerization. *J. Polym. Sci. Part A Polym. Chem.* **2020**, *58* (1), 42–47. https://doi.org/10.1002/pola.29504.

(4) Burchard, W. Solution Properties of Branched Macromolecules. *Adv. Polym. Sci.* **1999**, *143*, 113–194. https://doi.org/10.1295/kobunshi.47.816.